

Short note

Signature inversion in the yrare band of ^{119}Xe

C.-B. Moon^{1,a}, T. Komatsubara², Y. Sasaki², T. Jumatsu², K. Yamada², K. Satou², and K. Furuno²

¹ Department of Physics, Hoseo University, Chung-Nam 336-795, Korea

² Institute of Physics and Tandem Accelerator Center, University of Tsukuba, Ibaraki 305-8577, Japan

Received: 8 January 2002 / Revised version: 18 April 2002
Communicated by D. Schwalm

Abstract. Excited states of the ^{119}Xe nucleus have been studied by using in-beam γ -ray spectroscopy with the $^{107}\text{Ag} (^{16}\text{O}, \text{p}3\text{n}) ^{119}\text{Xe}$ fusion-evaporation reaction at a beam energy of 85 MeV. The level scheme of ^{119}Xe has been derived from γ - γ coincidence and γ - γ angular correlation analyses. We have, for the first time, established the second negative-parity favored and unfavored states built on the $11/2^-$ state, namely the yrare rotational bands in ^{119}Xe . In contrast to the behavior of the yrast bands where the favored states are lying lower in energy, the yrare favored states were observed to lie above the unfavored band. Such a signature inversion in ^{119}Xe is changed to be normal at $I = 12\hbar$.

PACS. 21.10.Re Collective levels – 23.20.Lv Gamma transitions and level energies – 27.60.+j $90 \leq A \leq 149$

The transitional nuclei, such as Xe and Ba in the $A = 120$ – 130 mass region, have attracted much attention since they provide useful information for the understanding of the polarizing effect of the valence quasiparticles on the nuclear shape. In this mass region the proton Fermi surface lies in the lower part of the $h_{11/2}$ subshell while the neutron Fermi surface lies in the $h_{11/2}$ midshell. The nuclei in this mass region are soft with respect to γ , the triaxiality parameter in the polar description of quadrupole shapes. Total Routhian surface (TRS) [1,2] and cranked shell model (CSM) [3,4] calculations suggest that these high- j valence particles exert a strong and specific driving force on the γ -soft core: particles in the lower part of the $h_{11/2}$ subshell favor a collectively rotating prolate shape ($\gamma \geq 0^\circ$ in the Lund convention), while those in the middle part of the $h_{11/2}$ subshell favor a collectively rotating triaxial shape ($\gamma \approx -30^\circ$).

In the even-mass Xe nuclei low-lying γ -vibrational bands have been observed that show a pronounced energy staggering between odd- and even-spin states [5,6]. This has been interpreted in terms of γ -soft nuclear potential in their low-lying states. In the odd-mass Xe isotopes, the unique-negative parity $h_{11/2}$ neutron orbital forms the yrast rotational band and their signature splitting features can be nicely described by cranking calculations. The second negative-parity rotational bands based on the high- j $h_{11/2}$ neutron orbital (called the yrare bands) were observed in ^{121}Xe [7], ^{123}Xe [8,9], and ^{125}Xe [10,11]. In con-

trast to the behavior of the yrast bands where the favored states are lying lower in energy, the yrare favored states are found to lie above the unfavored states, namely the signature splitting is inverted. Such a signature inversion in the yrare bands seems to be quite general in the light odd-mass Xe isotopes. With these features, we have investigated excited states of ^{119}Xe for observing the yrare negative-parity bands.

In this short note, we report the first observation of yrare bands in ^{119}Xe . The yrare bands were not observed in previous studies [12–16] of ^{119}Xe levels.

The level structure was studied with the $^{107}\text{Ag} (^{16}\text{O}, \text{p}3\text{n}) ^{119}\text{Xe}$ reaction at a beam of 85 MeV provided by the 12UD tandem accelerator at the University of Tsukuba. The target was a self-supporting foil of ^{107}Ag , 6.6 mg/cm² in thickness. The γ -ray spectra were measured with 11 high-purity (HP) Ge detectors with BGO anti-Compton shields (ACS). One of them was a low-energy photon (LEP) detector to ensure sensitivity for important low-energy transitions at the bottom parts of γ -ray cascades. Data were written onto 8 mm tapes (EXABYTE) for events in which two or more HP Ge detectors registered in prompt coincidence. Approximately 70 million events were collected. In the off-line analysis, the coincidence data were recalibrated to 0.5 keV/channel and sorted into 4096 by 4096 channel triangular matrices. Multipolarity information was extracted from the data by using the method of directional correlation of oriented states (DCO ratios). The coincidence events were sorted into

^a e-mail: cbmoon@office.hoseo.ac.kr

Table 1. γ -ray energies, intensities, DCO ratios, and spin-parity assignments to ^{119}Xe following the $^{107}\text{Ag} (^{16}\text{O}, \text{p}3\text{n}) ^{119}\text{Xe}$ reaction at a beam energy of 85 MeV.

E_γ (keV)	I_γ^a	R	Multipolarity	Assignment
176.0(2)	144.0(65)	0.7(1)	$E1$	$7/2^- \rightarrow 5/2^+$
398.8(2)	13.7(6)	1.0(2)	$E2$	$13/2^- \rightarrow 9/2^-$
401.7(2)	14.8(6)	0.4(1)	$E2/M1$	$13/2^- \rightarrow 11/2^-$
405.9(2)	100	1.0(1)	$E2$	$15/2^- \rightarrow 11/2^-$
559.3(4)	2.9(3)	1.0(2)	$E2$	$(17/2^-) \rightarrow (13/2^-)$
568.5(4)	2.6(3)	1.1(3)	$E2$	$(19/2^-) \rightarrow (15/2^-)$
575.4(3)	72.8(31)	1.0(1)	$E2$	$19/2^- \rightarrow 15/2^-$
580.6(2)	9.8(9)	0.4(2)	$E2/M1$	$17/2^- \rightarrow 15/2^-$
584.8(2)	17.8(8)	1.0(1)	$E2$	$17/2^- \rightarrow 13/2^-$
665.5(4)	1.2(2)	0.5(2)	$E2/M1$	$(23/2^-) \rightarrow 21/2^-$
679.4(3)	5.4(5)	1.1(2)	$E2$	$(21/2^-) \rightarrow (17/2^-)$
684.6(3)	6.4(6)	1.0(2)	$E2$	$(23/2^-) \rightarrow (19/2^-)$
704.5(4)	2.7(3)	0.6(2)	$E2/M1$	$(19/2^-) \rightarrow 17/2^-$
708.7(2)	47.8(22)	1.0(1)	$E2$	$23/2^- \rightarrow 19/2^-$
709.7(4)	1.3(2)		$E2/M1$	$(19/2^-) \rightarrow (19/2^-)$
716.6(4)	1.0(2)		$E2/M1$	$(15/2^-) \rightarrow (15/2^-)$
720.8(3)	3.7(4)	0.5(1)	$E2/M1$	$(15/2^-) \rightarrow (13/2^-)$
723.6(2)	12.8(6)	1.1(1)	$E2$	$21/2^- \rightarrow 17/2^-$
728.8(3)	6.3(5)	0.5(1)	$E2/M1$	$21/2^- \rightarrow 19/2^-$
759.3(4)	2.5(3)	0.7(1)	$E2/M1$	$(13/2^-) \rightarrow (11/2^-)$
769.8(4)	2.5(2)	0.9(2)	$E2$	$(27/2^-) \rightarrow (23/2^-)$
785.1(3)	7.3(6)	1.0(1)	$E2$	$(25/2^-) \rightarrow (21/2^-)$
818.0(3)	3.3(4)	1.1(3)	$E2$	$33/2^- \rightarrow 29/2^-$
820.7(2)	29.4(13)	1.0(1)	$E2$	$27/2^- \rightarrow 23/2^-$
832.3(2)	9.0(5)	1.0(1)	$E2$	$25/2^- \rightarrow 21/2^-$
846.7(3)	3.4(4)	1.2(3)	$E2$	$(29/2^-) \rightarrow (25/2^-)$
852.4(3)	5.7(5)	0.7(2)	$E2/M1$	$25/2^- \rightarrow 23/2^-$
895.5(2)	7.1(6)	1.0(1)	$E2$	$29/2^- \rightarrow 25/2^-$
910.7(2)	13.7(6)	1.0(1)	$E2$	$31/2^- \rightarrow 27/2^-$
912.7(3)	4.1(4)	0.5(1)	$E2/M1$	$(17/2^-) \rightarrow 15/2^-$
969.7 ^b (3)	5.7(6)	0.8(2)	$E2$	$35/2^- \rightarrow 31/2^-$
969.7 ^b (3)			$E2$	$39/2^- \rightarrow 35/2^-$
987.0(4)	2.1(2)	0.9(2)	$E2$	$43/2^- \rightarrow 39/2^-$
1016.7(4)	2.8(3)	0.6(1)	$M1/E2$	$(21/2^-) \rightarrow 19/2^-$
1094.1(4)	3.4(3)	0.4(2)	$M1/E2$	$(25/2^-) \rightarrow 23/2^-$

^a The values are normalized to 100% for the 405.9 keV transition.

^b γ -ray is a doublet.

an asymmetric matrix with energies of γ -rays detected in 5 detectors at 37° (or 143°) along one axis and energies of γ -rays detected in 5 detectors at 79° (or 101°) along the other axis. The intensities of $I_\gamma(37^\circ)$ and $I_\gamma(79^\circ)$ used to determine the DCO ratio, $R = I_\gamma(37^\circ)/I_\gamma(79^\circ)$, for the transitions of interest were extracted from spectra obtained by setting gates on the 37° and 79° axes of the γ - γ asymmetric matrix. In the present work, the DCO values were deduced from the gate on the stretched quadrupole transitions. Measured angular correlation ratios, $R = I_\gamma(37^\circ)/I_\gamma(79^\circ)$, are included in table 1 together with relative intensities and spin-parity assignments of the negative-parity states in ^{119}Xe . Figure 1 shows the partial level scheme of ^{119}Xe where only the negative-parity states are presented.

The favored yrast band (band 1), built on the $11/2^-$ state and its signature partner, unfavored yrast band

(band 2), were already known in the previous works [12–15]. In the present work, we confirmed all states up to the $43/2^-$. In a recent work by Scraggs *et al.* [15], this favored yrast band was extended up to $83/2^-$.

Bands 3 and 4, to which we assign negative parity, were identified in the present work. The population intensity for bands 3 and 4 is estimated to be 11% and 18%, respectively relative to that of the $15/2^-$ – $11/2^-$ 406 keV transition in band 1. The favored yrare states (band 3), are less populated than the unfavored yrare states (band 4). Band 4 is connected to the yrast favored states through several interband transitions, namely the 759, 913, 1017, 1094 keV γ -rays while band 4 is connected to both the yrast favored and unfavored states. Interband transitions from band 3 are rather strongly populated to the unfavored yrast band than to the favored yrast band. The proposed spin and parity assignments are essentially based

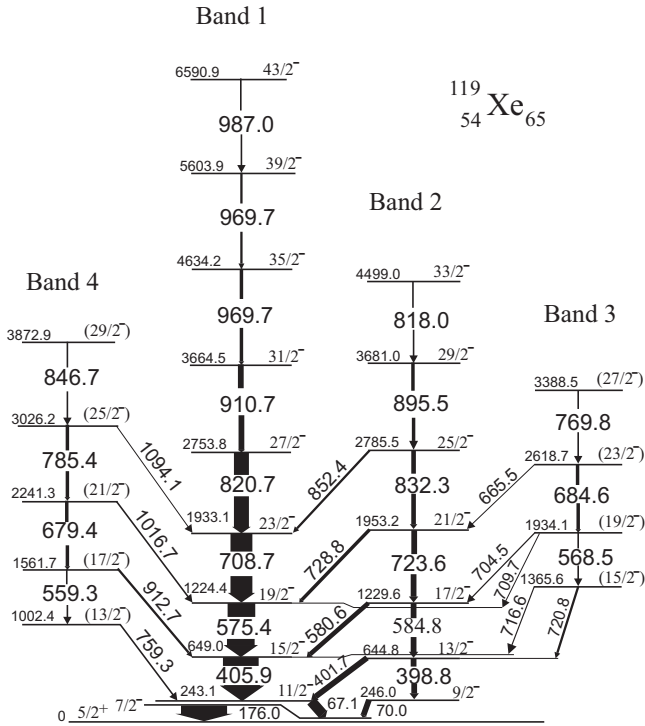


Fig. 1. The partial level scheme of ^{119}Xe deduced from the $^{107}\text{Ag} (^{16}\text{O}, \text{p}3\text{n}) ^{119}\text{Xe}$ reaction at a beam energy of 85 MeV. The widths of the arrows correspond to the intensities of the γ -ray transitions. Transition and excitation energies are given in keV.

on the multipolarity of the interband transitions connecting to the yrast bands 1 and 2. The DCO ratios indicate that the 913, 1017, and 1094 keV transitions connecting band 4 to the favored yrast band are $\Delta I = 1$ transitions with mixed $M1/E2$. The 721, 705, and 666 keV transitions connecting band 3 to band 2 are also of dipole character indicating $\Delta I = 1$ transitions with mixed $M1/E2$. So we propose that bands 3 and 4 should have negative parity.

The experimental level energies were transformed into a rotating frame of reference following the procedure outlined in refs. [3] and [4]. For subtracting a rotational reference, we used the Harris parameters $J_0 = 12\hbar^2 \text{MeV}^{-1}$ and $J_1 = 45\hbar^4 \text{MeV}^{-3}$, which provide a good reference for rotational frequencies below $\hbar\omega = 0.45 \text{MeV}$ [10, 11]. Figure 2 shows the plot of the extracted experimental Routhian e' (the quasiparticle energy in the rotating frame) as a function of the angular frequency $\hbar\omega$ for the yrast bands (bands 1 and 2) and the yrare bands (bands 3 and 4) in ^{119}Xe . Figure 3 shows the theoretical quasiparticle Routhians predicted by CSM calculations for the quasineutron configurations in ^{119}Xe . It is apparent that the configuration for yielding the yrast bands should originate from the $h_{11/2}$ neutron with the $[532]5/2$ Nilsson orbital.

In contrast to the feature of the large signature splitting in the yrast bands, the yrare bands have small signature splittings as shown in fig. 2. Furthermore, the favored yrare band (band 3) is lower in energy than the

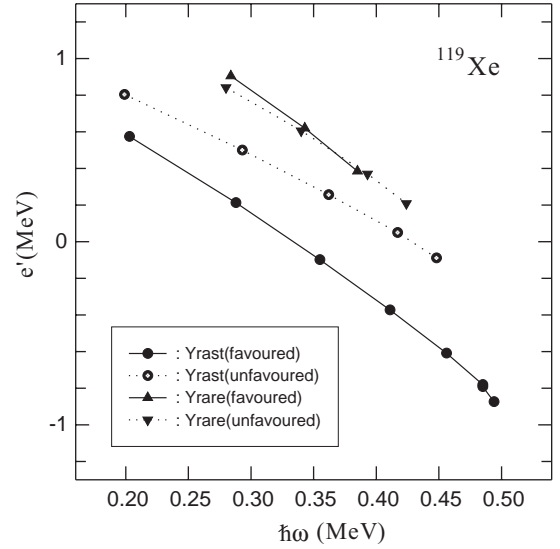


Fig. 2. Plots of the extracted experimental Routhian, e' as a function of the angular frequency $\hbar\omega$ for the yrast and yrare bands of ^{119}Xe . A rotational reference with the Harris parameters, $J_0 = 12\hbar^2 \text{MeV}^{-1}$ and $J_1 = 45\hbar^4 \text{MeV}^{-3}$ has been subtracted.

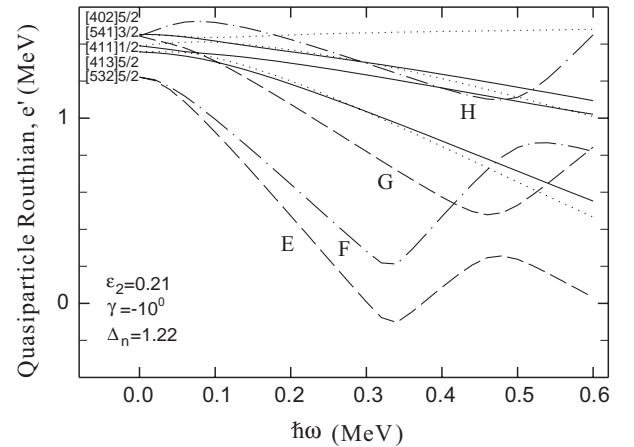


Fig. 3. Quasiparticle Routhians for ^{119}Xe with the following sets of deformation parameters: $\epsilon_2 = 0.21$, $\epsilon_4 = 0$, $\gamma = -10^\circ$, $\Delta_n = 1.22 \text{MeV}$. The parity and the signature, (π, α) of the levels are as follows: $(+, +1/2)$ solid lines, $(+, -1/2)$ dotted lines, $(-, -1/2)$ dashed lines, $(-, +1/2)$ dot-dashed lines.

unfavored band 4. Experimental Routhians e' shown in fig. 2 are compared with CSM calculations in fig. 3. Yrare states could not be explained as being associated with the second $h_{11/2}$ orbital, namely the G and F configurations. Instead, we propose that the yrare bands in ^{119}Xe as well as in other odd-mass Xe should be built on the $h_{11/2}$ neutron coupled to the γ bands in the neighboring even-even Xe core. In other words, the favored yrare states could be attributed to a neutron in $h_{11/2}$ orbital coupled to the even-spin γ band while the unfavored yrare ones being attributed to a neutron in $h_{11/2}$ orbital coupled to the odd-

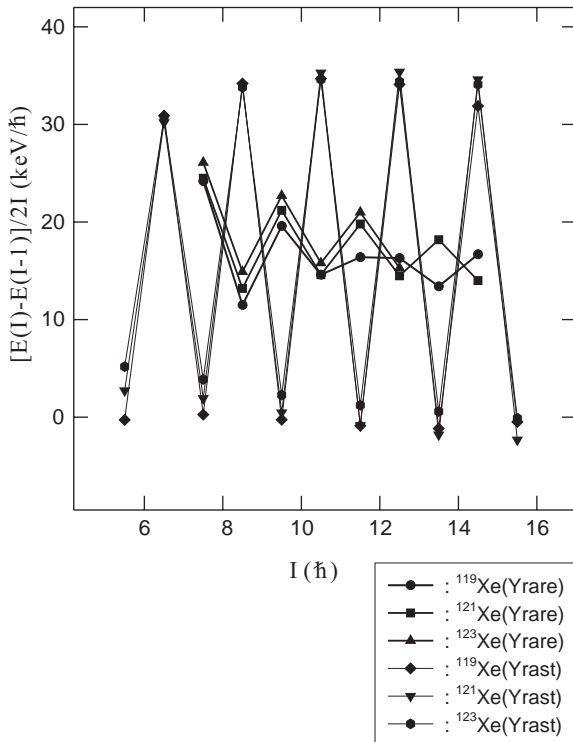


Fig. 4. Plots of the signature splittings of the negative-parity states in ^{119}Xe , ^{121}Xe , and ^{123}Xe as the form of $[E(I) - E(I - 1)]/2I$ against spin for the yrast and yrare bands.

spin γ band. The signature inversion in the yrare bands, however, cannot be reproduced by such a simple coupling of a quasiparticle with the γ vibration since the signature splitting in the γ bands is observed to be normal [6].

In order to make the signature splitting exhibited by the experimental energy visible, we plotted the quantity $[E(I) - E(I - 1)]/2I$ as a function of spin for the yrare bands observed in $^{119-123}\text{Xe}$ in fig. 4 where the yrast bands are included for comparisons. One can clearly see that the low-spin signatures for the unfavored yrare bands are inverted as compared to those in the yrast bands. Such a signature inversion in ^{119}Xe is changed to be normal at $I = 12\hbar$. The underlying physics involved in the signature inversion of the yrare bands has not been well understood. Using the rigid triaxial rotor plus particle (RTRP) model calculations, Liebertz *et al.* [17] interpreted the signature inversion for the yrare bands in ^{125}Xe to be caused by the large contribution from the core γ band. According to their interpretation, the signature inversion observed in ^{125}Xe can be attributed to the different contributions of the γ band to a neutron in the $h_{11/2}$ orbital.

Hamamoto [18] has pointed out that, for a certain nuclear shape deviating from axial symmetry, it is possible to expect an excitation spectrum where the second unfavored signature states are lying lower in their energy than the second favored signature states. Such a signature inversion can occur when the angular momentum of the collective rotation in the unfavored signature states may point to the direction that is quite different from the

one specified by the large moment of inertia for a certain triaxial intrinsic shape.

This work was supported by the Korea Research Foundation Grant (2000-015-DP0087).

References

1. R. Wyss, J. Nyberg, A. Johnson, R. Bengtsson, W. Nazarewicz, Phys. Lett. B **215**, 211 (1988).
2. W. Nazarewicz, R. Wyss, A. Johnson, Nucl. Phys. A **503**, 285 (1989).
3. R. Bengtsson, S. Frauendorf, Nucl. Phys. A **327**, 139 (1979).
4. R. Bengtsson, S. Frauendorf, F.-R. May, At. Data Nucl. Data Tables **35**, 15 (1986).
5. S. Törmänen, S. Juutinen, R. Julin, B. Cederwall, A. Johnson, R. Wyss, P. Ahonen, B. Fant, M. Matsuzaki, J. Nyberg, M. Piiparinen, S. Mitarai, J. Mukai, A. Virtanen, Nucl. Phys. A **572**, 417 (1994).
6. M. Serris, C.T. Papadopoulos, R. Vlastou, C.A. Kalfas, S. Kossionides, N. Fotiades, S. Harissopoulos, C.W. Beausang, M.J. Joyce, E.S. Paul, M.A. Bentley, S. Araddad, J. Simpson, J.F. Sharpey-Schafer, Z. Phys. A **358**, 37 (1997).
7. C.-B. Moon, T. Komatsubara, T. Shizuma, K. Uchiyama, T. Sasaki, K. Furuno, Eur. Phys. J. A **4**, 107 (1999).
8. A. Schmidt, I. Schneider, H. Meise, I. Wiedenhöver, O. Stuch, K. Jessen, D. Weisshaar, C. Schumacher, P. von Brentano, G. Sletten, B. Herskind, M. Bergstrom, J. Wrzesinski, Eur. Phys. J. A **2**, 21 (1998).
9. A. Gade, H. Meise, I. Wiedenhöver, A. Schmidt, A. Gelberg, P. von Brentano, Nucl. Phys. A **686**, 3 (2001).
10. Grandérath, D. Lieberz, A. Gelberg, S. Freund, W. Lieberz, R. Wirowski, P. von Brentano, R. Wyss, Nucl. Phys. A **524**, 153 (1991).
11. I. Wiedenhöver, J. Yan, U. Neuneyer, R. Wirowski, P. von Brentano, A. Gelberg, N. Yoshida, T. Otsuka, Nucl. Phys. A **582**, 77 (1995).
12. P. Chowdhury, U. Garg, T.P. Sjoreen, D.B. Fossan, Phys. Rev. C **23**, 733 (1981).
13. V. Barci, J. Gizon, A. Gizon, J. Crawford, J. Genevey, A. Plochocki, M.A. Cunningham, Nucl. Phys. A **383**, 309 (1982).
14. V.P. Janzen, M.P. Carpenter, L.L. Riedinger, W. Schmitz, D.G. Popescu, J.A. Cameron, J.K. Johansson, D.D. Rajnauth, J.C. Waddington, G. Kajrys, S. Monaro, S. Pilotte, Phys. Rev. C **39**, 2050 (1989).
15. H.C. Scraggs, E.S. Paul, A.J. Boston, J.F.C. Cocks, D.M. Cullen, K. Helariutta, P.M. Jones, R. Julin, S. Juutinen, H. Kankaanpää, M. Muikku, P.J. Nolan, C.M. Parry, A. Savelius, R. Wadsworth, A.V. Afanasjev, I. Ragnarsson, Nucl. Phys. A **640**, 337 (1998).
16. J. Genevey, A. Gizon, P.F. Mantica, W.B. Walters, G. Marguie, D. Bucurescu, the ISOLDE Collaboration, Phys. Rev. C **63**, 024321 (2001).
17. D. Lieberz, A. Gelberg, A. Grandérath, P. von Brentano, I. Ragnarsson, P.B. Semmes, Nucl. Phys. A **529**, 1 (1991).
18. I. Hamamoto, Nucl. Phys. A **520**, 297c (1990).